Pergamon

Geochimica et Cosmochimica Acta, Vol. 62, No. 10, pp. 1721–1733, 1998

0016-7037/98 $19.00 + .00

PII S0016-7037(98)00104-5

The strontium isotopic composition of Ordovician and Silurian brachiopods and conodonts: Relationships to geological events and implications for coeval seawater

HAIRUO QING,[1,*] CHRISTOPHER R. BARNES,[2] DIETER BUHL,[3] and JAN VEIZER[1,4]

[1]Ottawa-Carleton Geoscience Centre, University of Ottawa, Ottawa, Ontario K1N 6N5, Canada
[2]School of Earth and Ocean Sciences, University of Victoria, Victoria, British Columbia V8W 3P6, Canada
[3]Institut für Geologie, Ruhr Universität, 44780 Bochum, Federal Republic of Germany

(*Received October* 15, 1997; *accepted in revised form February* 4, 1998)

ABSTRACT—One hundred and fifty-six $^{87}Sr/^{86}Sr$ ratios were measured from Ordovician and Silurian brachiopod shells, marine calcite cements, and conodonts in order to establish the secular strontium isotope curve for the coeval seawater. Preservation of the brachiopod shell material has been evaluated by petrographic and geochemical criteria and only the well preserved internal secondary layer of the shells has been utilized for strontium isotope measurements. The results document a gradual decrease in $^{87}Sr/^{86}Sr$, from 0.7091 to 0.7087, from Tremadoc to Llandeilo, a sharp decline to 0.7078 during the late Llandeilo-early Caradoc; little change during Caradoc and the Ashgil; and a steady rise to 0.7087 through the Silurian. These long-term (10^7 yr) variations, with magnitudes in the range of 10^{-3}, are interpreted to be controlled primarily by continental collisional tectonics and its associated erosion and weathering.

The gradual decrease in $^{87}Sr/^{86}Sr$ ratio during the Early Ordovician may record the reduction in uplift and weathering rates due to waning of the Pan-African orogenies. The rapid decline near the Llandeilo/Caradoc boundary suggests a strong hydrothermal flux likely due to increased sea-floor spreading and a possible superplume event. The latter may have caused the prominent transgressive phase, the largest in the Phanerozoic, which would have muted continental flux input. Although the Caradoc was the main interval for the Taconic Orogeny, its impact on the Sr continental flux may have been delayed until the early Llandovery. This effect, complemented by reworking of glacial deposits near the Ordovician-Silurian boundary and enhanced by phases of the Silurian Salinic Orogeny, may have combined to give the progressive increase in the strontium isotope ratio through the Silurian. The scale and directionality of these changes makes the strontium isotope curve valuable for dating and correlation purposes.

1. INTRODUCTION

Strontium isotopic composition of marine carbonate minerals, if not altered during diagenesis, reflects the isotopic composition of seawater at the time of deposition, and such data indicate that $^{87}Sr/^{86}Sr$ ratio has varied systematically during the Phanerozoic (Burke et al., 1982). These variations result mostly from waxing and waning of the following major fluxes: radiogenic $^{87}Sr/^{86}Sr$ input due to subaerial weathering of continental crust, delivered principally via dissolved load of rivers; nonradiogenic $^{87}Sr/^{86}Sr$ flux that results from water/rock interactions at midoceanic ridges and from submarine alteration of basalts; and removal of Sr via precipitation and sedimentation, mostly by marine carbonates (e.g., Faure, 1986). Secular variations in the $^{87}Sr/^{86}Sr$ of seawater during geologic history can, therefore, provide valuable information for understanding the dynamics of the Earth system and can serve as an important baseline in the course of investigation of stratigraphy, petrology, diagenesis, and genesis of mineral deposits in sedimentary basins (Veizer, 1989).

The long oceanic residence time of Sr (~4 m.y.) and the rapid mixing rate of the oceans (10^3 yr) have caused the strontium isotope ratio of seawater to be globally homogeneous at any given time, as documented by identical $^{87}Sr/^{86}Sr$ ratios for coeval marine carbonates (e.g., Burke et al., 1982) and by measurements of modern seawater (Elderfield, 1986). This enables utilization of the seawater strontium isotopic curve for dating and correlation purposes, particularly for sparsely fossiliferous sequences. For example, Ludwig et al. (1988) were able to show that the sharp rises in $^{87}Sr/^{86}Sr$ at Enewetak atoll correlate with disconformities caused by subaerial erosion, whereas intervals with little change correspond to times of rapid accumulation of shallow water carbonates. This technique is most useful for dating Cenozoic sediments, where the curve is steep and unidirectional (DePaolo, 1986), but similar steep slopes have been documented also for earlier geologic history (cf. Burke et al., 1982).

Detailed knowledge of $^{87}Sr/^{86}Sr$ of ancient seawater is also crucial for deconvolution of the sedimentary and diagenetic histories of sedimentary basins. Such information, in turn, can help to interpret geologic events, such as dolomitization and mineralization in sedimentary basins (e.g., Banner et al., 1988; Mountjoy et al., 1992; Saller, 1984; Swart et al., 1987). Strontium isotopes can also serve as tracers of subsurface fluid movement and as indicators of connectivity of conduit systems, aquifers, or hydrocarbon reservoirs (Connolly et al., 1990; Qing and Mountjoy, 1992, 1994). Furthermore, strontium isotopes have also been utilized to investigate the origin and timing of gangue minerals in ore deposits (e.g., Kessen et al., 1981; Kesler et al., 1983, 1988; Barbieri et al., 1987; Ruiz et al., 1988).

The earlier systematic studies of Paleozoic sedimentary car-

**Present address:* Department of Geology, Royal Holloway, University of London, Egham Surrey TW20 0EX, England (ging@gl.rhbnc.ac.uk).

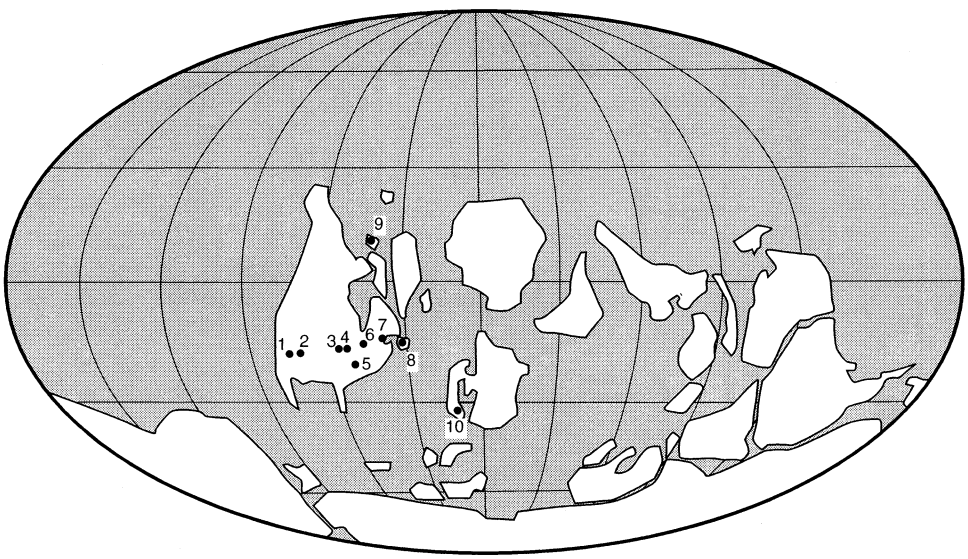

Fig. 1. Paleogeographic reconstruction for the Middle Ordovician based on Scotese and McKerrow (1990). Black dots indicate sample locations. Dot 1 corresponds to the approximate location of Nevada; 2 Utah; 3 Indiana; 4 Ohio; 5 Tennessee; 6 Ontario; 7 Anticosti Island; 8 Newfoundland; 9 Arctic; and 10 United Kingdom (modified after Qing and Veizer, 1994).

bonates succeeded in delineation of the secular patterns for strontium isotopes of Phanerozoic seawater that had a resolution of $\sim 10^7$ yr (e.g., Peterman et al., 1970; Veizer and Compston, 1974; Burke et al., 1982). For Ordovician and Silurian, the subject of the present study, the earlier published data were based primarily on whole rock samples (Burke et al., 1982; Gao and Land, 1991; Gao et al., 1996; Denison et al., 1997), although some measurements have been obtained from conodonts (Bertram et al., 1992; Ruppel et al., 1996; Holmden et al., 1996). Since whole rocks inevitably contain not only the primary marine components precipitated from ambient seawater, but also diagenetic cements that may have precipitated from fluids of different strontium isotopic compositions (see James and Choquette, 1990; Choquette and James, 1990), the resulting strontium isotope values are only averages for the constituting phases (e.g., Banner et al., 1988; Gao and Land, 1991). The main objectives of this paper are, therefore, (1) to refine the strontium isotope curve for the Ordovician and Silurian seawater, utilizing monomineralic low-Mg calcitic brachiopod shells, marine calcite cements, and conodonts, (2) to compare these results with the previously published data, and (3) to search for possible causes that could have generated the observed isotopic patterns.

2. MATERIALS USED FOR RECONSTRUCTION OF THE STRONTIUM ISOTOPE AGE CURVE

The bulk of the samples in this study comprises articulate brachiopods and conodonts. These samples were collected from localities in Laurentia, at paleolatitudes less than 30° (Fig. 1). Their locations, stratigraphic assignment, and generic identification are summarized in Appendices 1 and 2. For the purposes of this paper, the standard British stage/series nomenclature is used even though many of the samples come from North America. The absolute chronology is based on Harland et al. (1990).

The isotopic composition of ancient oceans can be deciphered from attributes of ancient chemical and biochemical precipitates. Brachiopod shells and conodonts are believed to represent the most suitable study material, particularly for the Paleozoic era, because of their abundance, stratigraphic utility, and low-Mg calcitic and phosphatic composition. The shell of articulate brachiopods is composed of low-Mg calcite and consists usually of the outer "primary" and the inner "secondary" layer. The primary layer is finely granular, with a distinct lineation perpendicular to the shell surface. In contrast, the secondary layer consists of elongated calcitic fibres that are oriented at an angle to the shell surface (MacKinnon, 1974). For the Paleozoic, the biochemical carbonate phases commonly used for reconstruction of the isotopic curves were the entire brachiopod shells (e.g., Popp et al., 1986), but recently only well preserved "secondary" layers have been utilized (Diener et al., 1996; Bruckschen et al., 1995; Veizer et al., 1997). In contrast to brachiopods, marine calcite cements, although at times precipitated as low-Mg calcite (Carpenter et al., 1991; Johnson and Goldstein, 1993), were mostly original aragonite or high Mg-calcite that must have been diagenetically altered to more stable low-Mg calcite. Nevertheless, their original strontium isotopic values can apparently be inferred from projections of isotopic trends (e.g., Carpenter et al., 1991).

Conodonts are phosphatic remains of an extinct group of chordates (Aldridge et al., 1986; Conway-Morris, 1989) that yield the most detailed stratigraphic resolution of any Paleozoic fossil group. Because of this, they could potentially represent the best material for generation of high resolution strontium isotope curves for Paleozoic seawater. Furthermore, conodont elements are composed of apatite with Sr contents of several thousands ppm (Pietzner et al., 1968; Wright et al., 1984, 1990; Kürschner et al., 1992) and their original $^{87}Sr/^{86}Sr$ is, thus, relatively difficult to contaminate by extraneous Sr. In addition, some authors (e.g., Kolodny and Epstein, 1976; Karhu and Epstein, 1986) proposed that apatite is more resistant to postdepositional alteration than calcite. The reconnaissance strontium isotope work on conodonts by Kovach (1980, 1981), Keto and Jacobsen (1987), and Bertram et al. (1992), and the detailed study of Martin and Macdougall (1995), support their utility for anticipated research. Yet, where conodonts and brachiopods were sampled from the same beds, the $^{87}Sr/^{86}Sr$ of conodonts was either similar to, or more radiogenic than, that of the brachiopods (Diener et al., 1996; Holmden et al., 1996). Theoretical modelling (Ebneth et al., 1997) suggests that conodonts do exchange post-depositionally their Sr with the surrounding matrix, leading to an isotopic shift by about 1/3 of the distance between the two endmembers. As a result, in a suitable matrix, such as carbonates, the isotopic shift may be only marginal, while in shales it may be considerable. Nevertheless, taking sufficient precaution in selection of the material,

and considering their ubiquity and stratigraphic resolution, conodonts do appear a promising material for strontium isotopic study (Martin and MacDougal, 1995). All the conodonts used in this study were extracted from carbonates.

In order to avoid problems of stratigraphic correlation and age assignment, conodont samples were selected from a few long stratigraphic sections in relatively undeformed platformal sequences where earlier taxonomic and biostratigraphic studies had been completed. Lower Ordovician samples were selected from collections from the St. George Group, Port au Port Peninsula, western Newfoundland. This area has yielded abundant conodonts of CAI (conodont alteration index) 1.0 ranging from the base of the Ordovician to the uppermost Arenig (Ji and Barnes, 1994). Higher strata mark the collapse of this ancient continental margin and platform and the stratigraphy is less complete. For the uppermost Arenig to basal Caradoc interval, conodonts were obtained from the Eleanor River, Bay Fiord and lower Thumb Mountain formations of the Franklinian miogeocline, southern Devon Island, Canadian Arctic Archipelago (Barnes, 1974; Carson, 1980; Barnes et al., 1981). These conodonts have a CAI of 1.5–2.0 and were recovered from subhorizontal strata. The basal Caradoc to upper Ashgill interval was represented by samples from the Black River and Trenton groups and carbonates in the overlying Collingwood, Lorraine and lower Queenston formations in southern Ontario where the CAI is 1.5–2.5 (Schopf, 1966; Barnes et al., 1978, 1981; Legall et al. 1982). The uppermost Ashgill to uppermost Llandovery was sampled from the Ellis Bay, Becscie, Gun River, Jupiter, and Chicotte formations on Anticosti Island, Quebec. The subhorizontal carbonates yield conodonts with a CAI of 1.0 (Nowlan and Barnes, 1981, 1987; McCracken and Barnes, 1981; Fåhraeus and Barnes, 1981; Uyeno and Barnes, 1983; Barnes 1988). Finally, for the Wenlock and Ludlow intervals of the Silurian, we used samples from the type areas of the Welsh Borderlands, U.K., from reference collections made by Barnes from sections visited with the Silurian Subcommission on Stratigraphy (e.g., Aldridge 1985; Holland and Bassett, 1989). Conodont CAI values of CAI 2.0–2.5 were reported by Aldridge (1985). No samples from the Upper Silurian Pridoli Stage were included in this study.

3. SAMPLE PREPARATION AND ANALYTICAL PROCEDURES

The collected brachiopod shells were small (0.5–2 cm) with thin shells (0.1–1 mm), particularly the early Ordovician ones. In order to avoid contamination from the matrix and/or from altered shell material by "dental drill" technique, we have used the preparation technique for brachiopod samples that was developed by the research group at the Ruhr University in Bochum (see Bruckschen et al., 1995; Diener et al., 1996; Veizer et al., 1997). The selected brachiopod shells were examined under transmitted light microscope and by cathodoluminescence (CL). The CL equipment used was a Technosyn 8200 MKII model, with settings at 10kV and 0.5 mA. Some shell fragments were also studied by scanning electron microscopy (SEM).

Complementary to textural examination, the state of preservation of the brachiopod shells (secondary layer only) was further evaluated using trace element chemistry. This analytical work was performed in the laboratories of the Ottawa-Carleton Geoscience Centre, utilizing Thermal-Jarrell Ash ATOMSCAN25 inductively coupled argon plasma sequential spectroscopy (ICP-AES). 15 to 20 mg of sample were digested in 15 mL of 8% HCl and analyzed for their Sr, Na, K, Fe, and Mn contents. The detection limits for Sr, Na, Mn, and Fe were 1, 50, 1, and 60 ppm, respectively. The reproducibility for duplicates was better than three relative percent. The results are listed in Appendix 1.

For separation of conodonts, 2–6 kg of visually unaltered samples were washed, crushed, and then dissolved in 5% acetic acid. Remains were washed with distilled water and decanted at intervals of 2–3 days. The sieved 80 μm-2 mm fraction was dried at 50°C. Clean conodonts with CAI of 1.0–2.5 were hand-picked under a binocular microscope. For strontium isotope measurements, one to three large, or up to ten small conodonts, all of the same genus were washed in distilled water by ultrasound and dissolved in 2 mL of 2.5 N HCl, in preparation for the ion exchange columns.

The NBS 987 and USGS EN-1 standard reference materials were used in the strontium isotope ratio measurements. For the time period of the analyses the mean of 23 NBS 987 measurements was 0.710238 ± 0.0000007 (2 standard deviation) and the mean of 15 USGS EN-1was 0.709170 ± 0.000007 (2 standard deviation). The NBS 987 is in form of a purified Sr solution (25 ng/μL) and was directly measured whereas the EN-1 carbonate powder had to pass through the chemical Sr separation before measurement. All standards and samples were loaded onto Re single filaments applying 2 μL of loading solution slightly modified after Birck (1986). The measured $^{87}Sr/^{86}Sr$ ratio was normalized to a value of 8.375209 for the $^{88}Sr/^{86}Sr$ ratio. The number of collected ratios per measurement was $n = 100$. The strontium isotope ratios were determined with a Finnigan MAT 262 multicollector TIMS using 3 of 7 available Faraday-cups in a peak jumping mode to compensate for a time depending change in Faraday-cup efficiencies. Since the actual $^{87}Rb/^{85}Rb$ ratio cannot be detected during a Sr measurement, a correction with a fixed $^{87}Rb/^{85}Rb$ ratio is not recommended. Instead of a correction, an upper limit for a tolerated ^{85}Rb signal was set to 5×10^{-5} Volt of ^{85}Rb with respect to a four to five Volt signal of ^{88}Sr. All measurements exceeding this limit were rejected. The average absolute blank for Sr (including chemicals, ion-exchange columns, and loading blank) did not exceed 8.5×10^{-3} ng. In total, forty-five brachiopod shells, ninety-eight conodont samples, and thirteen marine cements were analyzed for strontium isotopes.

4. SAMPLE SCREENING

4.1. Brachiopod Samples

4.1.1. Textural evaluation

In order to select the "best" preserved brachiopod shells, thin sections of brachiopods were examined under transmitted light and subsequently by cathodoluminescence (CL). As a rule, the unaltered shells consist of nonluminescent fibrous layers with no visible dissolution and cementation features (cf. Popp et al., 1986). Scanning electron microscope (SEM) studies confirmed the generally good preservation of the original brachiopod fabric, but dissolution features have been observed even in some nonluminescent samples (Fig. 2), indicating that they too may have experienced some diagenetic alteration (cf. Rush and Chafetz, 1990; Banner and Kaufman, 1994). Previous studies indicated that diagenetic alteration of brachiopod shells is most severe in the primary prismatic layer at its surface, while the volumetrically dominant secondary layer usually remains well preserved (Qing and Veizer, 1994; Diener et al., 1996). In order to minimize the role of diagenetic alteration, we employed all the above techniques for sample selection and analyzed only the nonluminescent "secondary" layer of the selected shells.

Due to the scarcity of early Ordovician (Tremadoc) articulate brachiopods, we could not find well preserved brachiopod shells for this time interval. Two Tremadoc brachiopods submitted for strontium isotopic analyses have visible diagenetic features, such as dissolution and recrystallization. Under the microscope, no primary fibrous structure was observed. In addition, the lime matrix in which these brachiopods were embedded is strongly recrystallized. The strontium isotopic values for these two Tremadoc brachiopods (Appendix 1) were, therefore, excluded from further consideration.

4.1.2. Geochemical evaluation

In addition to textural evaluation, trace elements were used as supplementary criteria for evaluation of brachiopod preservation. In general, diagenetic alteration leads to depletions in Sr and Na and enrichments in Mn and Fe (cf. Veizer, 1983). Figure 3 shows the plots of Sr, Mn, and iron vs. strontium isotopes. In all these plots, the brachiopod samples were of the same taxon, age, and location, and they show no recognizable pattern of post-depositional trace element redistribution with strontium isotope variations (Fig. 3). While the bulk of our samples has Sr and Na contents similar to those of Recent brachiopods (Fig. 4), the Fe and Mn contents of some specimens are much higher (Fig. 5), suggesting possible alteration by late-stage diagenetic processes. As a precautionary step, we have eliminated those brachiopods that have less than 800 ppm Sr or 500 ppm Na, as well as those with more than 800 ppm Fe, or 500 ppm Mn from further consideration. These, together with samples eliminated by textural criteria,

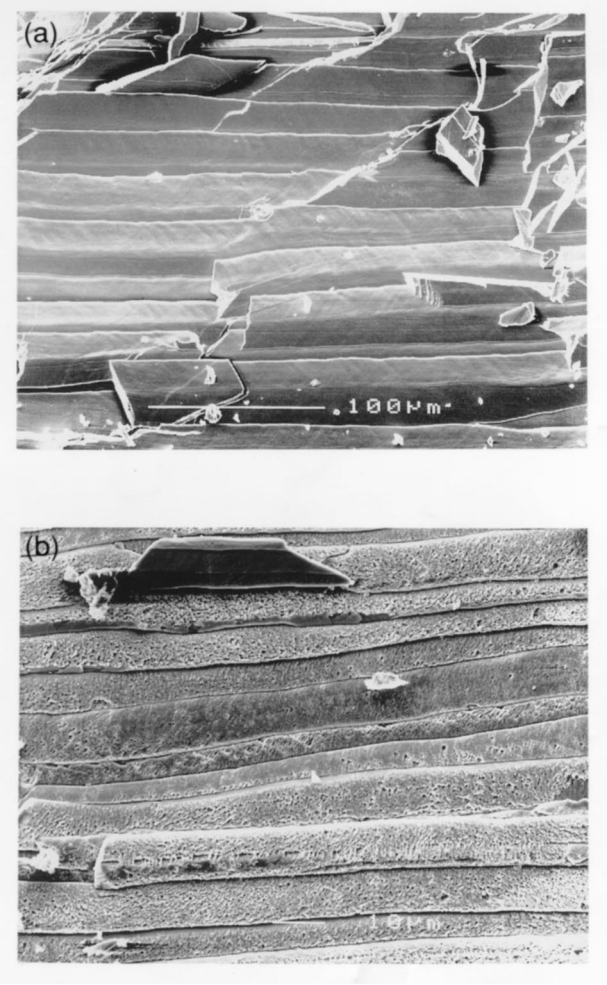

Fig. 2. SEM of brachiopod shell fragments. (a) Well-preserved secondary fibrous layer of brachiopod shell from the Ellis Bay Formation (Hirnantian), Anticosti Island (sample 18-1). (b) Slightly altered brachiopod shell with micro dissolution vugs from the Laval Formation (Llandeilo), Ontario (sample 12-6; from Qing and Veizer, 1994).

account for nineteen (or 42%) of the forty-five brachiopod samples analyzed for strontium isotopes.

4.2. Conodont Sample

Previous work on conodonts with variable CAI (Bertram et al., 1992; Kürschner et al., 1992; Holmden et al., 1996) showed that coeval samples with CAI higher than 2.5 had considerably greater dispersions in their strontium isotope values (1–2 x 10^{-4}) than their better preserved counterparts with CAI of 1–2 (2 x 10^{-5}). In addition, samples with high CAI usually had more radiogenic values. Taking this into account, we used conodonts with CAI in the range of 1.0–2.5. In total, ninety-eight conodont samples were analyzed. A few samples represent duplicates to check for strontium isotopic variations between elements of the same species or between different species within the same sample. Such variations tended to be within instrumental analytical errors.

5. TEMPORAL TREND

The overall temporal trend for strontium isotopes based on Ordovician brachiopods and marine cements and on Ordovician and Silurian conodonts is presented in Fig. 6. Together, they define a curve with far less scatter than that developed by Burke et al. (1982) using whole rock samples. For the reasons outlined by Veizer and Compston (1974) we utilize the least radiogenic values to constrain the strontium isotope trends for the Ordovician and Silurian seawater. The presently defined strontium isotope trend documents oscillations at ~ 3–5 x 10^7 yr frequency and 10^{-3} magnitude (Fig. 6).

The conodont data for the interval from the base of the Tremadoc (base of Ordovician) to upper Llandeilo (Fig. 6) display a gradual and steady decline from strontium isotope values of 0.7091–0.7087. The range of variation between different conodonts from the same sample is typically less than 0.0001. No acceptable brachiopod data are available for the Tremadoc. Brachiopod samples from the Arenig and Llanvirn show values similar to conodonts, or are slightly more radiogenic, with a wider dispersion (up to 0.0002) for coeval samples. The brachiopod values from the Llandeilo are about 0.0002 less radiogenic than those of coeval conodonts.

A major decline of strontium isotopes is evident from the upper Llandeilo to the lower Caradoc (Fig. 6). The data for conodonts and brachiopods are similar and both indicate a rapid change to less radiogenic values, from 0.7087 in the upper Llandeilo to 0.7078 in the lower Caradoc. The data points show only a small scatter, usually less than 0.0001. This remarkable change of ~0.001 (from 0.7087 to 0.7078) appears to occur within about 5 m.y. This dramatic excursion merits further examination with more intensive sampling through about 10 m.y. interval across the Llandeilo-Caradoc boundary. The low values (~ 0.7078) are maintained through the Caradoc and Ashgill and little modification to the trend is seen at the end of the Ordovician (Fig. 6). The $^{87}Sr/^{86}Sr$ ratios of our Caradoc samples from 445 to 457 m.y. are similar to those measured from contemporaneous whole rocks by Gao et al. (1996). We have no explanation for aberrant radiogenic measurements in the Caradoc that come from conodonts from the Thumb Mountain and Bay Fiord formation in the Arctic.

Through the Llandovery and Wenlock stages of the Lower Silurian, the trend reverses to more radiogenic values of 0.7087 by the upper Wenlock (Fig. 6). The Silurian portion of our strontium isotope trend, as defined by the results obtained from conodonts, is in general agreement with Silurian trend based on results acquired from whole rocks (Denison et al., 1997) and conodonts (Ruppel et al., 1996) and is only slightly more radiogenic than the new data set of Azmy (1996) that is based on Silurian brachiopods.

6. DISCUSSION

The strontium isotopic composition of seawater is determined primarily by the balance between radiogenic Sr delivered to the oceans via continental weathering (global average riverine $^{87}Sr/^{86}Sr$ ~0.7119; Palmer and Edmond, 1989) and relatively unradiogenic Sr released by mid-ocean ridge hydrothermal systems ($^{87}Sr/^{86}Sr$ about 0.7035; Palmer and Elderfield, 1985). An increase in continental erosion rate would, theoretically, increase the $^{87}Sr/^{86}Sr$ ratio of seawater, whereas an increase in hydrothermal activity should cause the opposite effect. The secular variations in strontium isotopic values of seawater through geologic time are caused mainly by the waxing and waning of the Sr mass and/or isotope fluxes from these two sources.

The "continental" flux should be higher after periods of orogenesis and continental suturing, presumably because of increased erosion following uplift (Clauer, 1976; Richter et al., 1992). Such scenario has been proposed to explain the continuous ^{87}Sr enrichment during the most recent 100 m.y. (Spooner, 1976). The "mantle" flux, on the other hand, may increase during times of enhanced seafloor spreading, plume/superplume activity, and continental rifting. The hydrothermal flux of Sr from mid-oceanic ridges in the geological past is believed to have been proportional to the rate of seafloor spreading. Fast spreading should correspond to high ridge

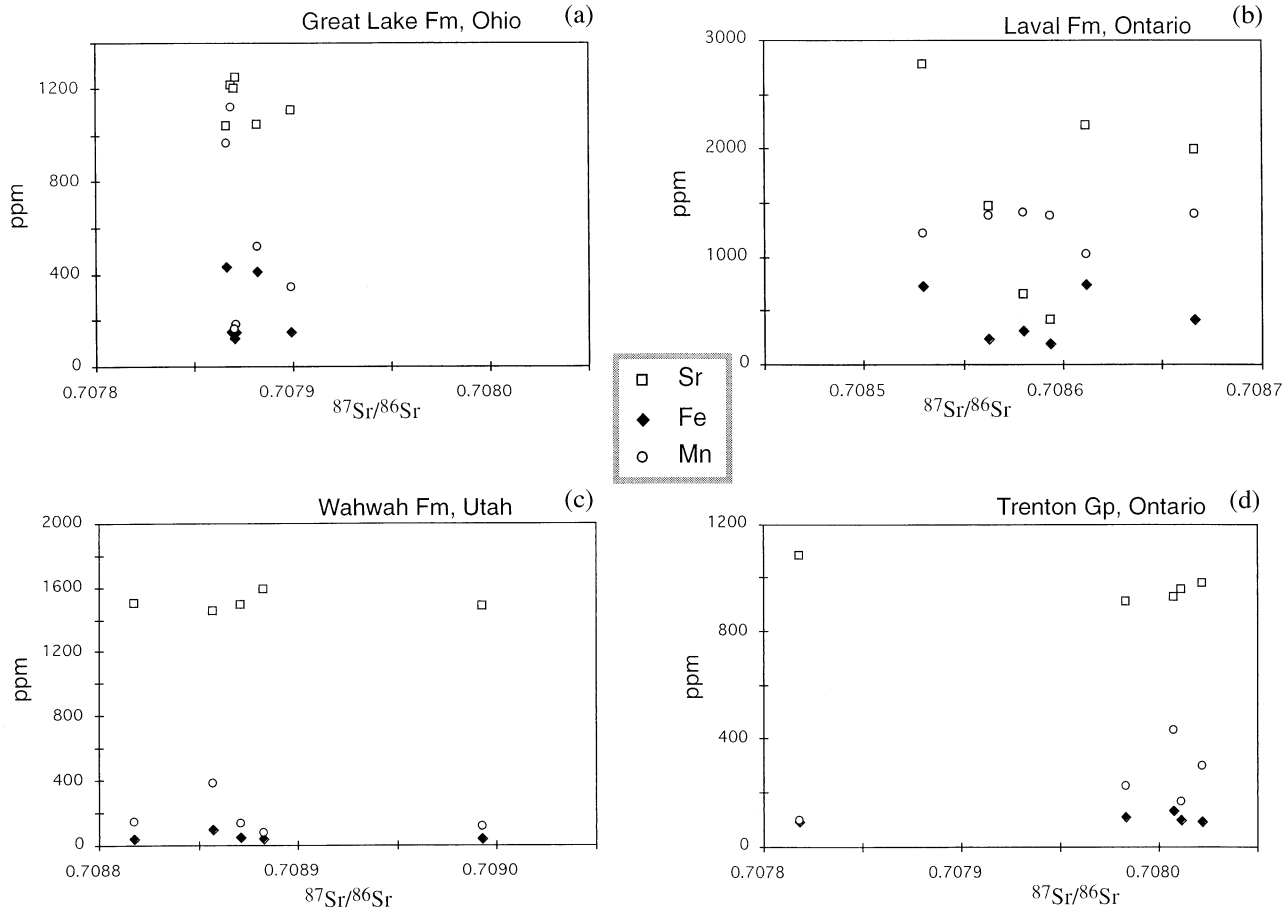

Fig. 3. Scatter diagrams of Sr (squares), Mn (circles), and Fe (diamonds) vs. $^{87}Sr/^{86}Sr$ ratios on brachiopods. (a) Plot of the Ashgill *Platystrophia* sp samples from the Great Lake Formation, Ohio; (b) Plot of Llandeilo *Mimella vulgaris* from the Laval Formation, eastern Ontario; (c) Plot of Arenig *Hesperonomia* sp. of the Wahwah Formation, Utah; (d) Plot of Caradoc *Strophomena* samples from the Trenton Group of southern Ontario.

volume, hence transgression onto cratons (coupled with reduction of exposed continental areas), and a decline in strontium isotopic ratios. This trend should be further enhanced by additional mantle Sr contributions from plumes and superplumes, although this is not evident for the Sr values of the mid Cretaceous for which a superplume has been postulated (Larson, 1991). Conversely, the $^{87}Sr/^{86}Sr$ ratio of seawater may increase during episodes of continental glaciation (Armstrong, 1971) when mechanical erosion and frost-shattering may accelerate the transfer of continental Sr to the oceans. The onset of a rapid increase in $^{87}Sr/^{86}Sr$ ratio of seawater, some 60 m.y. ago, apparently coincides with a low sea-level stand and the onset of Antarctic glaciation (De Paolo, 1986). Intervals of high atmospheric CO_2 should also enhance chemical weathering of continental rocks. Worsley and Kidder (1991) have argued for a feedback loop between the rate of chemical weathering and the cratonic area submerged. Yet, despite the fact that strontium isotopic geochemistry of the oceans is now fairly well understood, the causes of any particular fluctuation, especially for the Paleozoic Era, must be interpreted with caution.

Figure 6 juxtaposes our strontium isotope curve with the extent of continental deformation (intensity of continental collisional tectonics), the sea-level changes, and major geologic events. The gradual decrease in seawater $^{87}Sr/^{86}Sr$ ratios during Early Ordovician times is a continuation of a trend that commenced in the Late Cambrian, subsequent to culmination of seawater $^{87}Sr/^{86}Sr$ ratio at about 0.7093 during the Middle to earliest Late Cambrian (Montanez et al., 1996). This culmination was interpreted by Montanez et al. (1996) as a result of the climax of mountain building and of associated unroofing and weathering of ^{87}Sr-rich high-grade metamorphic zones during the Pan-African orogeny (ca. 800–500 m.y.; Miller, 1983). The Early Ordovician decrease in seawater $^{87}Sr/^{86}Sr$ ratios may thus record a gradual reduction in the topographic relief and in weathering rates that characterized the waning phases of Pan-African orogenies. Furthermore, the sea level was moderately high and broad areas of the cratons were flooded (Ross and Ross, 1992), thus potentially suppressing the radiogenic riverine Sr flux to the oceans.

The most intriguing strontium isotope excursion is the dramatic decline from 0.7087 to 0.7078 from the Llandeilo to early Caradoc. This excursion needs to be addressed by further, more intense, sampling. Tentatively, we propose two explanations but have no evidence to support either. First, the rapid change

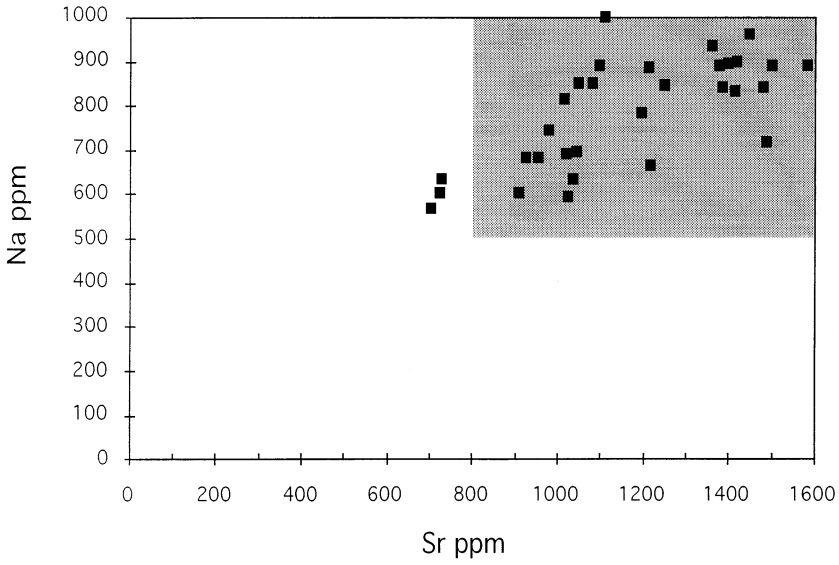

Fig. 4. Scatter diagram of Sr and Na concentrations in Ordovician brachiopods. Shaded area for recent brachiopods, which have Sr contents from 800 to 2,000 ppm and Na contents from 500 to 3,700 ppm (Morrison and Brand, 1986).

could represent a hiatus or misassignment of ages. Second, it may have been caused by a combined effect of: (1) reduced continental flux due to the tranquillity of continental orogenies and/or transgression; and (2) increased mantle flux resulting from a possible superplume event. The early Caradoc change is synchronous with a major transgression, the largest in the Phanerozoic in terms of cratonic area submerged (Ross and Ross, 1992). Such a transgression would shut down much of the continental erosional input and is likely to be a reflection of high sea-floor spreading rates. The scale of the transgression, combined with the absence of magnetic reversals for much of the Ordovician (Johnson et al., 1995), the postulated high levels of CO_2 (Berner, 1991), the widespread black shales (Leggett, 1980) all led Barnes et al. (1995) to propose a superplume event, possibly initiated in the Llanvirn and peaking in the Caradoc. Such a superplume event could have generated the required nonradiogenic oceanic flux.

The low $^{87}Sr/^{86}Sr$ values of the Caradoc continue through the Ashgill (Fig. 6) with little change. The terminal Ordovician continental glaciation, with 2–4 principal glacial phases (Barnes 1986; Brenchley et al., 1991,1994) over a brief period of 4 m.y., but concentrated in the Hirnantian Stage ($\sim$ 0.5 m.y.) at the end of the Ashgill, heralds the termination of the low $^{87}Sr/^{86}Sr$ values. The subsequent progressive increase in the $^{87}Sr/^{86}Sr$ values through the Silurian may be interpreted as a reflection of two principal influxes of continental material. First, the Llandovery transgression would have redeposited and incorporated much of the continental

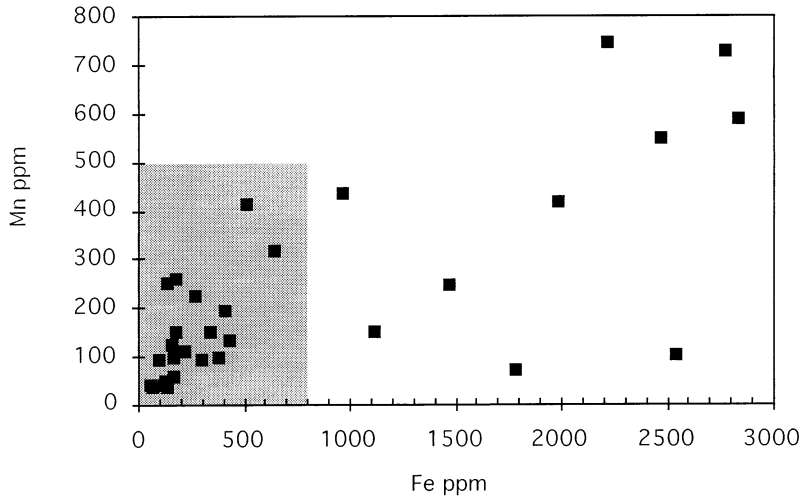

Fig. 5. Scatter diagram of Mn and Fe concentrations in Ordovician brachiopods. Shaded area for recent brachiopods, which have Mn from 5 to 500 ppm and Fe from 20 to 800 ppm (Morrison and Brand, 1986).

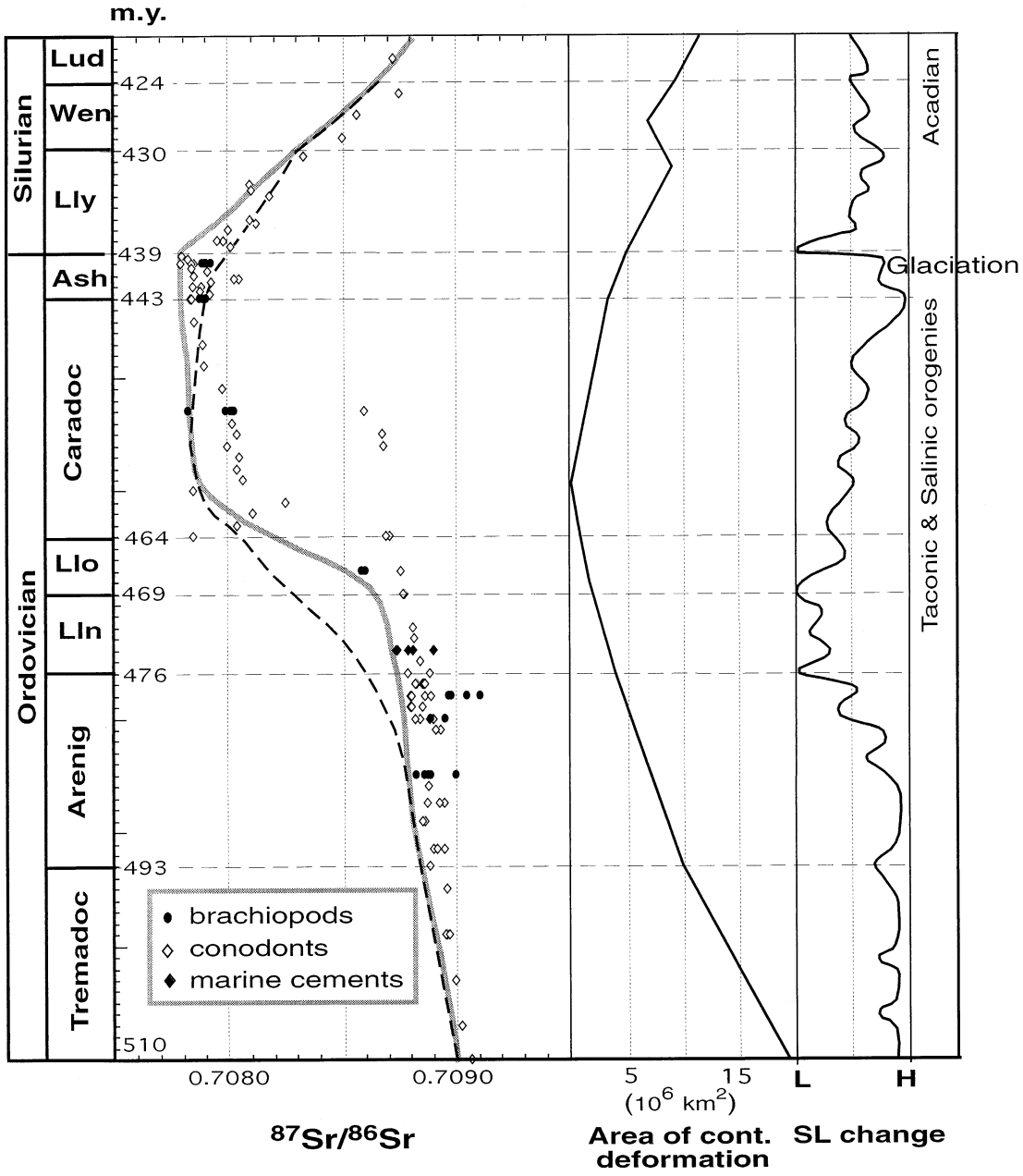

Fig. 6. $^{87}Sr/^{86}Sr$ values of Ordovician and Silurian brachiopods, marine cements, and conodonts plotted according to the best available stratigraphic information. The time scale of Harland et al. (1990) is used. The area of continental deformation is based on the information from Richter et al. (1992), the sea-level curve of Ordovician and Silurian is based on Ross and Ross (1992) and Johnson and Mckerrow (1991), respectively. Brachiopods are represented as dots, conodonts as open diamonds, and marine cements as solid diamonds. The shaded line contours the least radiogenic strontium isotopic values and dash line represents strontium isotopic values from Burke et al. (1982). Lud stands for Ludlow; Wen for Wenlock; Lly for Llandovery; Ash for Ashgill; Llo for Llandeilo; and Lln for Llanvirn.

weathering products generated by the Ashgill glaciation in Gondwana and peri-Gondwana terranes as well as by the mechanical and chemical weathering of the widely exposed cratons during the Ashgill regression. Second, an increase in riverine Sr flux and/or its $^{87}Sr/^{86}Sr$ ratio could have been caused by the climax of arc-continent collision events (the Taconian Orogeny) that resulted in exhumation and chemical weathering of ^{87}Sr-rich high-grade metamorphic rocks at the eastern margin of Laurentia. Although the Caradoc was the main interval for the Taconic Orogeny, its impact on the Sr continental flux may have been delayed until the early Llandovery because a substantial thickness of marine carbonates needed to be stripped from emerging highland before exposing the more radiogenic basement rocks (cf. Rich-

ter et al., 1992). Uplift of Taconic mountains along the eastern seaboard of the North America is indicated also by detrital influx from orographic sources, culminating in deltaic progradation during the Ashgill (Witzke, 1990). In the Wenlock to Ludlow interval, new continental input may have developed in response to the early phases of the Acadian Orogeny. There has been a recent recognition of the greater magnitude of the early Silurian Salinic Phase (Dunning et al., 1990; Cawood et al., 1994) that represents the initial suturing of Baltica from Laurentia.

7. CONCLUSIONS

156 Ordovician and Silurian brachiopod shells, marine calcite cements, and conodonts were analyzed for strontium isotopes in order to refine the strontium isotope curve for the Ordovician and Silurian seawater. Preservation of the brachiopod shell material was examined by petrographic and geochemical criteria and only the well preserved internal secondary layer of the shells were utilized for strontium isotope measurements.

The measurements define secular trend of decreasing strontium isotope values, from 0.7091 to 0.7078, from Tremadoc to early Caradoc, with most of the decline near the Llandeilo-Caradoc boundary; little changed from the Caradoc to the Ashgill; and a steady increase through the Silurian to 0.7087 in the Ludlow. This long-term trend (10^7 yr), with a magnitude in the range of 10^{-3}, is interpreted to be controlled primarily by continental collisional tectonics that is accompanied by enhanced erosion and weathering. The gradual decrease in strontium isotope values from Tremadoc to middle Llanvirn coincides with a steady decrease in continental deformation, with the minimum in the Caradoc and Ashgill. In the same way, the steady increase in strontium isotope values during the Silurian coincides with increasing continental deformation. Due to the rapid rate of change, particularly during the Silurian, the seawater strontium isotope curve has a considerable potential for chemostratigraphic applications.

Acknowledgments—We acknowledge donation of samples by T. E. Bolton (Geological Survey of Canada, Ottawa), H. J. Hoffman (University of Montreal, Montreal), E. Landing (New York Geological Survey, Albany), J. F. Miller (S.W. Missouri State University, Springfield) and J. B. Waddington (Royal Ontario Museum, Toronto). This study was financially supported by the Natural Sciences and Engineering Research Council of Canada, the Deutsche Forochungsgemeinschaft, and Royal Holloway University of London. We appreciate the comments from Dr. M. F. Thirlwall and two anonymous reviewers.

REFERENCES

Aldridge R. J. (1985) Conodonts of the Silurian System from the British Isles. In *a Stratigraphical Index of British Conodonts* (ed. A. C. Higgins and R. L. Austin), pp. 68–92. Ellis Horwood.

Aldridge R. J., Briggs D. E. G., Clarkson E. N. K., and Smith M. P. (1986) The affinities of conodonts — new evidence from the Carboniferous of Edinburgh, Scotland. *Lethaia* **19,** 279–291.

Armstrong R. L. (1971) Glacial erosion and the variable composition of strontium in seawater. *Nature Phys. Sci.* **230,** 132–33.

Azmy K. (1996) Isotopic composition of Silurian brachiopods: implication for coeval seawater. PhD Thesis, Univ. Ottawa.

Banner J. L. and Kaufman J. (1994) The isotopic record of ocean chemistry and diagenesis preserved in non-luminescent brachiopods from Mississippian carbonate rocks, Illinois and Missouri. *Geol. Soc. Amer. Bull.* **106,** 1074–1082.

Banner J. L., Hanson G. N., and Meyers W. J. (1988) Fluid-rock interaction history of regionally extensive dolomites of the Burlington-Keokuk Formation (Mississippian): isotope evidence. In *Sedimentology and Geochemistry of Dolostones* (ed. V. Shukla & P.A. Baker); *Spec. Publs Soc. Econ. Paleont. Miner.* **43,** 97–113.

Barbieri M., Bellanca A., Neri R., and Tolomeo L. (1987) Use of strontium isotopes to determine the sources of hydrothermal fluorite and barite from northwestern Sicily (Italy). *Chem. Geol.* **66,** 273–78.

Barnes C. R. (1974) Ordovician conodont biostratigraphy of the Canadian Arctic. In *Proc. Symposium on Geology of the Canadian Arctic* (ed. J. D. Aitken and D. J. Glass), pp. 221–240. Geol. Assoc. Canada

Barnes C. R. (1986) The faunal extinction event near the Ordovician-Silurian boundary: a climatically induced crisis. In *Global Bioevents* (ed. O.H. Walliser); *Lect. Notes Earth Sci.* **8,** 121–126. Springer-Verlag.

Barnes C. R. (1988) Stratigraphy and paleontology of the Ordovician-Silurian boundary interval, Anticosti Island, Quebec. In *a Global Analysis of the Ordovician-silurian Boundary* (ed. L. R. M. Cocks and R. Rickards); *Brit. Mus. (Nat. Hist.) Bull.* **43,** 195–219.

Barnes C. R., Telford P. G., and Tarrant G. A. (1978) Ordovician and Silurian conodont biostratigraphy, Manitoulin Island and Bruce Peninsula, Ontario, Michigan Basin. *Geol. Soc. Spec. Paper* **3,** 68–71.

Barnes C. R., Norford B. S., and Skevington D. (1981) The Ordovician System in Canada. Correlation chart and explanatory notes. *Intl. Union Geol. Sci. Publ. 8.*

Barnes C. R., Fortey R. A., and Williams S. H. (1995) The pattern of global bio-events during the Ordovician Period. In *Global Events and Event Stratigraphy in the Phanerozoic* (ed. O. H. Walliser), pp. 139–172. Springer-Verlag.

Berner R. A. (1991) A model for atmospheric CO_2 over Phanerozoic time. *Amer. J. Sci.* **291,** 339–376.

Bertram C. J., Elderfield H., Aldridge R. J., and Conway-Morris S. (1992) $^{87}Sr/^{86}Sr$, $^{143}Nd/^{144}Nd$ and REEs in Silurian phosphatic fossils. *Earth Planet. Sci. Lett.* **113,** 239–249.

Birck J. L. (1986) Precision K-Rb-Sr isotopic analysis: application to Rb-Sr Chronology. *Chem. Geol.* **56,** 73–83.

Brenchley P. J., Romano M., Young T. P., and Storch P. (1991) Hirnantian glaciomarine diamictites-Evidence for the spread of glaciation and its effect on Ordovician faunas. In *Advances in Ordovician Geology* (ed. C. R. Barnes and S. H. Williams); *Geol. Surv. Canada Paper 90-9,* 325–336.

Brenchley P. J. et al. (1994) Bathymetric and isotopic evidence for a short-lived Late Ordovician glaciation in a greenhouse period. *Geology* **22,** 295–298.

Bruckschen P., Bruhn F., Meijer J., Stephan A., and Veizer J. (1995) Diagenetic alteration of calcitic fossil shells: Proton microprobe (PIXE) as a trace element tool. *Nucl. Inst. Methods Phys. Res. B* **104,** 427–431.

Burke W. H., Denison R. E., Hetherington E. A., Koepinck R. B., Nelson H. F., and Otto J. B. (1982) Variation of seawater $^{87}Sr/^{86}Sr$ throughout Phanerozoic time. *Geology* **10,** 516–519.

Carpenter S. J., Lohmann K. C., Holden P., Walter L. M., Huston T. J., and Halliday A. N. (1991) $\partial^{18}O$ values, $^{87}Sr/^{86}Sr$ and Sr/Mg ratios of Late Devonian abiotic marine calcite: implications for the composition of ancient seawater. *Geochim. Cosmochim. Acta* **55,** 1991–2010.

Carson D. M. (1980) Canadian-Whiterockian (Ordovician) conodont biostratigraphy of the Arctic Platform, Southern Devon Island, Eastern Canadian Arctic Archipelago. Ph.D. dissertation, Univ. Waterloo.

Cawood P. A., Dunning G. R., Lux D., and van Gool J. A. M. (1994) Timing of peak metamorphism and deformation along the Appalachian margin of Laurentia in Newfoundland: Silurian, not Ordovician. *Geology* **22,** 339–402.

Choquette P. W. and James N. P. (1990) Limestones—The burial diagenetic environment. In Diagenesis (ed. MciLreath & Morrow); *Geosci. Canada Reprints Ser.* **4,** 75–111.

Clauer N. (1976) Géochimie isotopiques du strontium des milieux sédmientaires. Application à la géochronologie de la couverture du craton ouest-africain. *Mém. Sci. Géol. Strasbourg* **45,** 1–126.

Connolly C. A., Walter L. M., Baadsgaard H., and Longstaffe F. J.

(1990) Origin and evolution of formation waters, Alberta Basin, Western Canada Sedimentary Basin. 2. Isotope systematics and water mixing. *Appl. Geochem.* **5,** 397–413.

Conway-Morris S. (1989) Conodont paleobiology: recent progress and unsolved problems. *Terra Nova* **1,** 135–150.

Denison R. E., Koepnick R. B., Burke W. H., Hetherington E. A., and Fletcher A. (1997) Construction of the Silurian and Devonian seawater $^{87}Sr/^{86}Sr$ curve. *Chem. Geol.* **140,** 109–121.

De Paolo D. J. (1986) Detailed record of the Neogene strontium isotopic evolution of seawater from DSDP site 5908. *Geology* **14,** 103–106.

Diener A., Ebneth S., Veizer J., and Buhl D. (1996) Strontium isotope stratigraphy of the Middle Devonian: brachiopods and conodonts. *Geochim. Cosmochim. Acta* **60,** 639–652.

Dunning G. R. et al. (1990) Silurian orogeny in the Newfoundland Appalachians. *J. Geol.* **98,** 895–913.

Elderfield H. (1986) Strontium isotope stratigraphy. *Palaeogeogr. Palaeoclimatol. Palaeoecol.* **57,** 71–90.

Ebneth S. Deiner A., Buhl D., and Veizer J. (1997) Strontium isotope systematics of conodonts: Middle Devonian, Eifel Mts., Germany. *Palaeogeogr. Palaeoclimatol. Palaeoecol.* **132,** 79–96.

Fåhraeus L. E. And Barnes C. R. (1981) Conodonts from the Becscie and Gun River Formations (Lower Silurian) of Anticosti Island, Quebec. In *Stratigraphy and Paleontology Field Meeting, Anticosti-Gaspe, Quebec, 1981* (ed. P. J. Lesperance), pp. 165–172. Intl. Union Geol. Sci.

Faure G. (1986) *Principles of Isotope Geology*. Wiley.

Gao G. And Land S. L. (1991) Geochemistry of Cambro-Ordovician Arbuckle limestone, Oklahoma: implications for diagenetic $\partial^{18}O$ alteration and secular $\partial^{13}C$ and $^{87}Sr/^{86}Sr$ variation. *Geochim. Cosmochim. Acta* **55,** 2911–2920.

Gao G., Dworkin S. I., Land L. S., and Elmore R. D. (1996) Geochemistry of Late Ordovician Viola limestone, Oklahoma: implications for marine carbonate mineralogy and isotopic compositions. *J. Geol.* **104,** 359–367.

Harland W. B., Armstrong R. L., Cox A. V., Craig L. E., Smith A. G., and Smith D. G. (1990) *a Geological Time Scale 1989.* Cambridge Univ. Press.

Holland C. H. And Bassett M. G. (ed.) (1989) A Global Standard for The Silurian System. Natl. Mus. Wales Geol. Ser. No. 9, Cardiff.

Holmden C., Creaser R. A., Muehlenbachs K., Bergstrom S. M., and Leslie S. A. (1996) Isotopic and elemental systematics of strontium and neodymium in 454 Ma biogenic apatites: implications for paleoseawater studies. *Earth. Planet. Sci. Lett.* **142,** 425–437.

James N. P. And Choquette P. W. (1990) Limestones - The meteoric diagenetic environment. In *Diagenesis* (ed. I. A. MciLreath and D. W. Morrow); *Geosci. Canada Reprints Ser.* **4,** 35–73.

Ji Z. and Barnes C. R. (1994) Lower Ordovician conodont taxonomy, phylogeny, and biostratigraphy of the St. George Group of Port au Port Peninsula, western Newfoundland, Canada. *Palaeontogr. Canadiana* **11,** 1–149.

Johnson H. P., Van Patten D., Tivey M., and Sager W. W. (1995) Geomagnetic polarity reversal rate for the Phanerozoic. *Geophys. Res. Letts.* **22,** 231–234.

Johnson W. J. and Goldstein R. H. (1993) Cambrian seawater preserved as inclusions in marine low-magnesium calcite cement. *Nature* **232,** 335–337.

Karhu J. and Epstein S. (1986) The implication of the oxygen isotope records in coexisting cherts and phosphates. *Geochim. Cosmochim. Acta* **50,** 1745–1756.

Kesler S. E., Ruiz J., and Jones L. M. (1983) Strontium-isotopic geochemistry of fluorite mineralization (Coahuila, Mexico). *Isot. Geosci.* **1,** 65–75.

Kesler S. E., Jones L. M., and Ruiz J. (1988) Strontium isotopic geochemistry of Mississippi Valley-type deposits, east Tennessee: Implications for age and source of mineralizing brines. *Geol. Soc. Amer. Bull.* **100,** 1300–7.

Kessen K. M., Woodruff M. S., and Grant N. K. (1981) Gangue mineral $^{87}Sr/^{86}Sr$ ratios and the origin of Mississippi Valley-type mineralization. *Econ. Geol.* **76,** 913–20.

Keto L. and Jacobsen S. B. (1987) Neodymium and strontium isotopic variations of Early Paleozoic oceans. *Earth Planet. Sci. Lett.* **84,** 27–41.

Kolodny Y. and Epstein S. (1976) Stable isotope geochemistry of deep sea cherts. *Geochim. Cosmochim. Acta* **40,** 1195–1209.

Königshof P. (1991) Conodont colour alteration adjacent to a granitic intrusion, Harz Mountains. *N. Jb. Geol. Paläont. Mh.* **2,** 84–90.

Kovach J. (1980). Variations in the strontium isotopic composition of seawater during Palaeoxoic time determined by analysis of conodonts. *GSA Abstr. Prog.* **12,** 465 (abstr.).

Kovach J. (1981) The strontium content of conodonts and possible use of the strontium concentrations and strontium isotopic composition on conodonts for correlation purposes. *GSA Abstr. Prog.* **13,** 285 (abstr.).

Kürschner W., Becker R. T., Buhl D., and Veizer J. (1992) Strontium isotopes in conodonts: Devonian/Carboniferous transition, the northern Rhenish Slate Mountains, Germany. *Ann. Soc. Géol. Belgique* **115,** 595–621.

Larson R. C. (1991) Latest pulse of the Earth: evidence for a mid-Cretaceous superplume. *Geology* **19,** 540–550.

Legall R. D., Barnes C. R., and Macqueen R. W. (1982) Organic metamorphism, burial history and hotspot development, Paleozoic strata of southern Ontario-Quebec, from conodont and acritarch alteration studies. *Bull. Canada Petrol. Geol.* **29,** 492–539.

Leggett J. K. (1980) British Lower Paleozoic black shales and their palaeo-oceanographic significance. *J. Geol. Soc., London* **137,** 139–156.

Ludwig K. R., Halley R. B., Simmons K. R., and Peterman Z. E. (1988) Strontium isotope stratigraphy of Enewetak Atoll. *Geology* **16,** 173–77.

Mackinnon D. I. (1974) The shell structure of spiriferide brachiopoda. *Bull. British Museum* **25,** 187–261.

Martin E. E. and Macdougall J. D. (1995) Strontium and neodymium isotopes at the Permian/Triassic boundary: a record of climate change. *Chem. Geol.* **125,** 73–99.

McCracken A. D. and Barnes C. R. (1981) Conodont biostratigraphy and paleoecology of the Ellis Bay Formation, Anticosti Island, Quebec, with special reference to Late Ordovician-Early Silurian chronostratigraphy and the systemic boundary. *Geol. Surv. Canada Bull.* **329,** 51–134

Miller R. M. (1983) The Pan-African orogen of Southwest African/Namibia. *Geol. Soc. South Africa Spec. Pub.* **11,** 431–515.

Montanez I. P., Banner J. L., Osleger D. A., Borg L. E., and Bosserman P. J. (1996) Integrated strontium isotope variations and sea level history of Middle to upper Cambrian platform carbonates: implications for the evolution of Cambrian seawater $^{87}Sr/^{86}Sr$. *Geology* **24,** 917–920.

Morrison J. O. and Brand U. (1986) Geochemistry of recent marine invertebrates. *Geosci. Canada* **13,** 237–254.

Mountjoy E. W., Qing H., and Mcnutt R. (1992) Strontium isotopic composition of Devonian dolomites, Western Canada: Significance as sources of dolomitizing fluids. *Appl. Geochem.* **7,** 57–75.

Nowlan G. S. and Barnes C. R. (1981) Late Ordovician conodonts from the Vaureal Formation, Anticosti Island, Quebec. *Geol. Surv. Canada Bull.* **329,** 1–49.

Nowlan G. S. and Barnes C. R. (1987) Thermal maturation of Paleozoic strata in eastern Canada from conodont colour alteration index (C.A.I.) data with implications for burial history, tectonic evolution, hotspot tracks and mineral and hydrocarbon potential. *Geol. Surv. Canada Bull.* **367,** 1– 47.

Palmer M. R. and Edmond J.M. (1989) The strontium isotope budget of the modern ocean. *Earth Planet. Sci. Lett.* **92,** 11–26.

Palmer M. R. and Elderfield H. (1985) Strontium isotopic composition of seawater over the past 75 Myr. *Nature* **314,** 526–28.

Peterman Z. E., Hedge C. E., and Tourtelot H. A. (1970) Isotopic composition of strontium in seawater throughout Phanerozoic time. *Geochim. Cosmochim. Acta* **34,** 105–20.

Pietzner H., Vahl J., Werner H., and Ziegler W. (1968). Zur chemischen Zusammensetzung und Micromorphologie der Conodonten. *Paleontographica* **128,** 115–152.

Popp B. N., Podosek F. A., and Anderson T. F. (1986) $^{87}Sr/^{86}Sr$ ratio in Permo-Carboniferous sea water from the analysis of well preserved brachiopod shells. *Geochim. Cosmochim. Acta* **50,** 1321–1328.

Qing H. and Mountjoy E. W. (1992) Large-scale fluid flow in the Middle Devonian Presqu'ile barrier, Western Canada Sedimentary Basin. *Geology* **20,** 903–906.

Qing H. and Mountjo E. W. (1994) Formation of coarsely crystalline, hydrothermal dolomite reservoirs in the Presqu'ile barrier, Western Canada Sedimentary Basin. *Amer. Assoc. Petroleum Geol. Bull.* **78,** 55–77.

Qing H. and Veizer J. (1994) Oxygen and carbon isotopic composition of Ordovician brachiopods: Implication for coeval seawater. *Geochim. Cosmochim. Acta* **58,** 4429–4442.

Richter F. M., Rowley D. B., and Depaolo D. J. (1992) Strontium isotope evolution of seawater: the role of tectonics. *Earth Planet. Sci. Lett.* **109,** 11–23.

Ross J. R. and Ross C. A. (1992) Ordovician sea-level fluctuations. In *Global Perspectives on Ordovician Geology* (ed. B. D. Webby and J. R. Laurie), pp. 327–335. Balkema.

Ruiz J., Richardson C. K., and Patchett P. J. (1988) Strontium isotope geochemistry of fluorite, calcite and barite in the Cave-in-Rock fluorite. *Econ. Geol.* **83,** 203–10.

Ruppel S. C., James E. W., Barrick J. E., Nowlan G. S., and Uyeno T. T. (1996) High resolution $^{87}Sr/^{86}Sr$ chemostratigraphy of the Silurian: implications for event correlation and strontium flux. *Geology* **24,** 831–834.

Rush P. F. and Chafetz H. S. (1990) Fabric-retentive, non-luminescent brachiopods as indicators of original $\partial^{13}C$ and $\partial^{18}O$ composition: a test. *J. Sediment. Petrol.* **60,** 968–981.

Saller A. H. (1984) Petrologic and geochemical constraints on the origin of subsurface dolomite, Enewetak atoll: an example of dolomitization by normal seawater. *Geology* **12,** 217–20.

Schopf T. J. M. (1966) Conodonts of the Trenton Group (Ordovician), Ottawa Valley, Canada. Ph.D. dissertation, Carleton University.

Scotese C. R. and McKerrow W. S. (1990) Revised world maps and introduction. In Palaeozoic Palaeogeography and Biogeography. *Geol. Soc. London Mem.* **12,** 1–21.

Spooner E. T. C. (1976) The strontium isotopic composition of seawater and seawater-oceanic crust interaction. *Earth Planet. Sci. Lett.* **31,** 167–74.

Swart P. K., Ruiz J., and Holmes C. W. (1987) Use of strontium isotopes to constrain the timing and mode of dolomitization of upper Cenozoic sediments in a core from San Salvador, Bahamas. *Geology* **15,** 262–65.

Uyeno T. T. and Barnes C. R. (1983) Conodonts of the Jupiter and Chicotte Formations (Lower Silurian), Anticosti Island, Quebec. *Geol. Surv. Canada Bull.* **355,** 1–49.

Veizer J. (1983) Chemical diagenesis of carbonates: Theory and application of trace element technique. In *Stable Isotopes in Sedimentary Geology* (ed. M. A. Arthur et al.); *SEPM Short Course* **10,** 3.1–3.100.

Veizer J. (1989) Strontium isotopes in seawater through time. *Ann. Rev. Earth Planet. Sci.* **17,** 141–167.

Veizer J. and Compston W. (1974) Composition of seawater during the Phanerozoic. *Geochim. Cosmochim. Acta* **38,** 1461–1484.

Veizer J. et al. (1997) Strontium isotope stratigraphy: Potential resolution and event correlation. *Pal. Pal. Pal.* **132,** 65–77.

Witzke B.J. (1990) Palaeoclimatic constraints for Palaeozoic palaeolatitudes of Laurentia and Euramerica. In Palaeozoic Palaeogeography and Biogeography. *Geol. Soc. Mem.* **12,** 57–73.

Worsley T. R. and Kidder D. L. (1991) First-order coupling of paleogeography and CO2, with global surface temperature and its latitudinal contrast. *Geology* **19,** 1161–1164.

Wright J., Seymour R. S. and Shaw H. F. (1984) REE and neodymium isotopes in conodont apatite: variations with geological age and depositional environment. *GSA Spec. Pap.* **196,** 325–340.

Wright J., Conca J. L., Repetski J. E., and Clark J. (1990) Microgeochemistry of some lower Ordovician Cordylodans from Jilin, China. *Cour. Forsch.-Inst. Senckenberg* **118,** 307–331.

Appendix 1. List of brachiopod and marine cement samples and analytical data. Trace elements are in ppm.

No	Strat.	Fm.	Description	Location	Assigned age (m.y.)	87Sr/86Sr	Sr	Fe	Mn	K	Na	I.R.%
18-1	Ash	Ellis Bay	*Velamo sp.*	Anticosti Is	440	0.707897	1097	59	37	30	890	0.00
18-2	Ash	Ellis Bay	*Velamo sp.*	Anticosti Is	440	0.707996	1048	1785	72	219	851	0.00
18-3	Ash	Ellis Bay	*Velamo sp.*	Anticosti Is	440	0.707921	1016	174	54	325	813	0.00
19-1	Ash	Ellis Bay	*Eospirigeria praendgis*	Anticosti Is	440	0.707888	1022	2544	99	342	689	0.00
19-2	Ash	Ellis Bay	*Eospirigeria praendgis*	Anticosti Is	440	0.707882						
19-3	Ash	Ellis Bay	*Eospirigeria praendgis*	Anticosti Is	440	0.707890						
17-1	Ash	Great Lake	*Platystrophia sp.*	Ohio	443	0.707882	1045	516	412	251	693	0.00
17-2	Ash	Great Lake	*Platystrophia sp.*	Ohio	443	0.707866	1037	967	432	225	634	0.00
17-3	Ash	Great Lake	*Platystrophia sp.*	Ohio	443	0.707899	1109	342	148	229	998	0.00
17-5	Ash	Great Lake	*Platystrophia sp.*	Ohio	443	0.707869	1213	1119	150	416	886	0.00
17-6	Ash	Great Lake	*Platystrophia sp.*	Ohio	443	0.707871	1252	184	149	244	844	0.00
17-7	Ash	Great Lake	*Platystrophia sp.*	Ohio	443	0.707870	1199	164	123	379	782	0.00
15-1	Crd	Trenton	*Strophomena*	Ontario	453	0.707983	908	225	109	178	603	0.02
15-2	Crd	Trenton	*Strophomena*	Ontario	453	0.708007	926	430	133	414	683	0.00
15-3	Crd	Trenton	*Strophomena*	Ontario	453	0.708011	957	166	95	101	684	0.00
15-4	Crd	Trenton	*Strophomena*	Ontario	453	0.707818	1083	99	91	382	848	0.00
15-5	Crd	Trenton	*Strophomena*	Ontario	453	0.708022	981	302	91	266	742	0.00
16-1	Crd	Trenton	*??*	Tennesse	453	0.707976	730	272	222	328	633	0.22
16-2	Crd	Trenton	*??*	Tennesse	453	0.708368	725	139	250	180	601	0.00
16-3	Crd	Trenton	*??*	Tennesse	453	0.707941	703	182	256	423	567	0.00
12-1	Llo	Laval Fm	*Mimella vulgaris*	Ontario	467	0.708594	1379	415	192	291	891	0.00
12-4	Llo	Laval Fm	*Mimella vulgaris*	Ontario	467	0.708530	1216	2782	727	146	663	0.02
12-5	Llo	Laval Fm	*Mimella vulgaris*	Ontario	467	0.708563	1386	1476	244	360	842	0.00
12-6	Llo	Laval Fm	*Mimella vulgaris*	Ontario	467	0.708666	1398	1985	415	417	893	0.04
12-7	Llo	Laval Fm	*Mimella vulgaris*	Ontario	467	0.708580	1415	647	316	300	832	0.05
12-8	Llo	Laval Fm	*Rostricellula raymondi*	Ontario	467	0.708612	1026	2220	743	251	592	0.01
26-2	Lln	t-Kanosh	*Anomalorthis sp.*	Utah	472	0.709270						
26-3	Lln	t-Kanosh	*Anomalorthis sp.*	Utah	472	0.709526						
26-4	Lln	t-Kanosh	*Anomalorthis sp.*	Utah	472	0.709077						
MC-1	Lln	Antelope Valley Ls.	Marine cement	Nevada	474	0.708738	275	105	150	231	164	0.00
MC-2	Lln	Antelope Valley Ls.	Marine cement	Nevada	474	0.708831						
MC-3	Lln	Antelope Valley Ls.	Marine cement	Nevada	474	0.709023	344	123	100	74	205	0.00
MC-4	Lln	Antelope Valley Ls.	Marine cement	Nevada	474	0.708811	384	258	87	22	122	0.00
MC-5	Lln	Antelope Valley Ls.	Marine cement	Nevada	474	0.709319	377	228	166	109	280	0.00
MC-6	Lln	Antelope Valley Ls.	Marine cement	Nevada	474	0.708742	360	235	75	202	245	0.00
MC-7	Lln	Antelope Valley Ls.	Marine cement	Nevada	474	0.708735	414	101	65	345	302	0.00
MC-8	Lln	Antelope Valley Ls.	Marine cement	Nevada	474	0.708787	328	357	68	12	206	0.00
MC-9	Lln	Antelope Valley Ls.	Marine cement	Nevada	474	0.708811	379	115	83	281	289	0.00
MC-10	Lln	Antelope Valley Ls.	Marine cement	Nevada	474	0.708899	336	65	84	201	259	0.00
MC-11	Lln	Antelope Valley Ls.	Marine cement	Nevada	474	0.708733	436	1038	307	633	297	0.00
MC-12	Lln	Antelope Valley Ls.	Marine cement	Nevada	474	0.708787	434	804	290	550	215	0.00
MC-13	Lln	Antelope Valley Ls.	Marine cement	Nevada	474	0.708841	405	857	499	591	164	0.00
10-1	Lln	m-Kanosh	*Anomalorthis sp.*	Utah	475	0.709049	1421	2477	549	545	896	0.04
10-3	Lln	m-Kanosh	*Anomalorthis sp.*	Utah	475	0.708909	1363	2839	586	312	932	0.03
25-1	Lln	b-Kanosh	*Anomalorthis sp.*	Utah	478	0.709041						
25-2	Lln	b-Kanosh	*Anomalorthis sp.*	Utah	478	0.709327						
25-3	Lln	b-Kanosh	*Anomalorthis sp.*	Utah	478	0.708963						
25-4	Lln	b-Kanosh	*Anomalorthis sp.*	Utah	478	0.708973						
25-5	Lln	b-Kanosh	*Anomalorthis sp.*	Utah	478	0.709101						
23-3	Arg	Juab	*Orthambonites sp.*	Utah	480	0.708881						
23-5	Arg	Juab	*Orthambonites sp.*	Utah	480	0.708945						
9-1	Arg	Wahwah	*Hesperonomia sp.*	Utah	485	0.708871	1489	133	47	125	717	0.00
9-2	Arg	Wahwah	*Hesperonomia sp.*	Utah	485	0.708993	1480	117	41	267	841	0.00
9-3	Arg	Wahwah	*Hesperonomia sp.*	Utah	485	0.708818	1500	143	34	365	890	0.00
9-4	Arg	Wahwah	*Hesperonomia sp.*	Utah	485	0.708883	1583	71	34	184	888	0.00
9-6	Arg	Wahwah	*Hesperonomia sp.*	Utah	485	0.708857	1450	380	96	466	962	0.00
5-1	Tre	Fillmore	*Hesperonomia sp.*	Utah	490	0.709550						
5-2	Tre	Fillmore	*Hesperonomia sp.*	Utah	490	0.709079						

Appendix 2. List of conodont samples and analytical data.

Sample No.	Strat Unit	*Species/element*	Location	Assigned age (m.y.)	87Sr/86Sr
E0009	L. Leint.	*Panderodus gracilis*	UK	422	0.708722
E0007	U. Bring.	*Panderodus gracilis*	UK	425	0.708752
E0004	Top Wenlock	*Panderodus gracilis*	UK	427	0.708563
E0002	Much Wenlock	*Panderodus gracilis*	UK	429	0.708498
E0020	Brassfield	*Panderodus gracilis*	UK	437	0.708001
E0023	Salamonie	*Panderodus gracilis*	Indiana	430.5	0.708332
E0021	Salamonie	*Panderodus gracilis*	Indiana	431.5	0.706327
(9715)A79P56	Jupiter	*Panderodus gracilis*	Anticosti	433	0.708093
(9701)A79P42	Jupiter	*Panderodus gracilis*	Anticosti	433.5	0.708103
(9693)A79P34	Jupiter	*Panderodus gracilis*	Anticosti	434	0.708179
(9663c)A79P4	Gun River	*Panderodus gracilis*	Anticosti	436	0.708093
(9682)A79P23	Gun River	*Panderodus gracilis*	Anticosti	436.5	0.708121
(9748)A79P81	Becscie	*Panderodus gracilis*	Anticosti	438	0.707949
(9735)A79P68	Becscie	*Panderodus gracilis*	Anticosti	438.5	0.708011
045	Manitoulin	*Panderodus gracilis*	Ontario	438	0.707970
039	Georgian Bay	*Panderodus gracilis*	Ontario	439.3	0.707799
027	Georgian Bay	*Panderodus gracilis*	Ontario	439.6	0.707823
023	Georgian Bay	*Phragmodus undatus*	Ontario	440	0.707848
023	Georgian Bay	*Phragmodus undatus*	Ontario	440	0.707793
023	Georgian Bay	*Panderodus gracilis*	Ontario	440	0.707841
020	Georgian Bay	*Phragmodus undatus*	Ontario	440.3	0.707837
EMC21	Georgian Bay	*Phragmodus undatus*	Ontario	440.6	0.707907
EMC19	Georgian Bay	*Phragmodus undatus*	Ontario	441	0.707851
EMC13	Georgian Bay	*Drepanodus suberectus*	Ontario	441.3	0.708047
EMC13	Georgian Bay	*Phragmodus undatus*	Ontario	441.3	0.708024
EMC8	Georgian Bay	*Phragmodus undatus*	Ontario	441.6	0.707922
EMC6	Georgian Bay	*Phragmodus undatus*	Ontario	442	0.707884
EMC2	Georgian Bay	*Phragmodus undatus*	Ontario	442.3	0.707877
C7	U. Whitby	*Phragmodus undatus*	Ontario	442.6	0.707917
102	L. Whitby	*Phragmodus undatus*	Ontario	443	0.707833
SC8	Bobcaygeon	*Phragmodus undatus*	Ontario	454	0.708017
SC1	Bobcaygeon	*Phragmodus undatus*	Ontario	455	0.708036
PA7	Bobcaygeon	*Panderodus gracilis*	Ontario	456	0.707992
PA1	Bobcaygeon	*Panderodus gracilis*	Ontario	457	0.708049
K20	Bobcaygeon	*Polycaulodus bidentatus*	Ontario	458	0.708034
N14	Bobcaygeon	*Panderodus gracilis*	Ontario	459	0.708062
N9	Gull River	*Polycaulodus bidentatus*	Ontario	460	0.707844
N6	Gull River	*Polycaulodus bidentatus*	Ontario	461	0.708248
U14	Gull River	*Drepanoistodus suberectus*	Ontario	462	0.708104
U4	Gull River	*Panderodus gracilis*	Ontario	463	0.708036
KM1	Shadow Lake	*Polycaulodus bidentatus*	Ontario	464	0.707847
9623	Allen Bay	*Panderodus gracilis*	Arctic	442	0.707845
363/8147	basal Allen Bay	*Panderodus gracilis*	Arctic	443	0.707842
9614	basal Irene Bay	*Panderodus gracilis*	Arctic	445	0.707848
352/8136	Thumb Mt.	*Panderodus gracilis*	Arctic	447	0.707889
350/8134	Thumb Mt.	*Panderodus gracilis*	Arctic	449	0.707894
347/8131	Thumb Mt.	*Panderodus gracilis*	Arctic	451	0.707974
342/8126	Thumb Mt.	*Panderodus gracilis*	Arctic	453	0.708597
338/8122	Thumb Mt.	*Panderodus gracilis*	Arctic	455	0.708678
335/8119	Thumb Mt.	*Drepanodus concavus*	Arctic	456	0.708679

Appendix 2. List of conodont samples and analytical data (continued).

Sample No.	Strat Unit	*Species/element*	Location	Assigned age (m.y.)	87Sr/86Sr
B32 C.C.	Bay Fiord	*Acontiodus curvatus*	Arctic	464	0.708710
B32 Ta	Bay Fiord	*Tricladiodus albus*	Arctic	464	0.708693
A27 E.P.	Bay Fiord	*Glyptoconus quadraplicatus*	Arctic	467	0.708757
A25 A.M.	Bay Fiord	*Oistodus multicorrugatus*	Arctic	469	0.708767
A25 E.P.	Bay Fiord	*Glyptoconus quadraplicatus*	Arctic	469	0.708773
A25 S.G.	Bay Fiord	*Striatodontus gracilis*	Arctic	469	0.708764
A21	Bay Fiord	*Acodus deltatus deltatus*	Arctic	472	0.708808
A19 E.P.	Bay Fiord	*Glyptoconus quadraplicatus*	Arctic	473	0.708814
A14 E.P.	Bay Fiord	*Glyptoconus quadraplicatus*	Arctic	475	0.708841
A10 E.P.	Eleanor River	*Glyptoconus quadraplicatus*	Arctic	476	0.708881
A12 A.D.	Bay Fiord	*Acodus deltatus deltatus*	Arctic	477	0.708856
A112 E.P.	Bay Fiord	*Glyptoconus quadraplicatus*	Arctic	477	0.708860
AO6 E.P.	Eleanor River	*Glyptoconus quadraplicatus*	Arctic	478	0.708889
AO1	Eleanor River	*Glyptoconus quadraplicatus*	Arctic	480	0.708902
E0038 (con)	Cow Head	*Periodon aculeatus*	Nfld.	476	0.708784
E0038 (brach)	Cow Head	Inarticulate brachiopod	Nfld.	476	0.709648
St.P.120	Cow Head	*P. acul. (aculeatus)*	Nfld.	477	0.708823
St.P.120	Cow Head	*P. acul. (oistod.)*	Nfld.	477	0.708854
St.P.120	Cow Head	*P. acul. (prioniod.)*	Nfld.	477	0.708821
St.P.99	Cow Head	*P. acul. (aculeatus)*	Nfld.	478	0.708796
St.P.99	Cow Head	*P. acul. (aculeatus)*	Nfld.	478	0.708861
St.P.99	Cow Head	*P. acul. (prioniod.)*	Nfld.	478	0.708803
St.P.94	Cow Head	*P. acul. (aculeatus)*	Nfld.	479	0.708797
St.P.94	Cow Head	*P. acul. (oistod.)*	Nfld.	479	0.708851
St.P.94	Cow Head	*P. acul. (prioniod.)*	Nfld.	479	0.708805
St.P.92	Cow Head	*P. acul. (aculeatus)*	Nfld.	480	0.708839
St.P.92	Cow Head	*P. acul. (oistod.)*	Nfld.	480	0.708881
St.P.92	Cow Head	*P. acul. (prioniod.)*	Nfld.	480	0.708818
St.P.81	Cow Head	*P. acul. (aculeatus)*	Nfld.	481	0.708934
St.P.81	Cow Head	*P. acul. (oistod.)*	Nfld.	481	0.708933
St.P.81	Cow Head	*P. acul. (prioniod.)*	Nfld.	481	0.708910
Z297	Catoche	*Acodus comptus*	Nfld.	486	0.708877
Z294B/3	Catoche	*Acodus comptus*	Nfld.	487.5	0.708947
Z294B/2	Catoche	*Glyptoconus quadraplicatus*	Nfld.	487.5	0.708874
Z294B/1	Catoche	*Oepikodus communis*	Nfld.	487.5	0.708926
Z2 77.2	Boat Hbr.	*Glyptoconus quadraplicatus*	Nfld.	489	0.708860
Z2 77.1	Boat Hbr.	*Glyptoconus quadraplicatus*	Nfld.	489	0.708854
Z2 65/3	Boat Hbr.	*Drepanodus concavus*	Nfld.	491.5	0.708902
Z2 65/2	Boat Hbr.	*Drepanodus concavus*	Nfld.	491.5	0.708947
Z2 65/1	Boat Hbr.	*Drepanodus concavus*	Nfld.	491.5	0.708918
Z2 47	Boat Hbr.	*Striatodontus prolificus*	Nfld.	493	0.708882
Z2 37B	Boat Hbr.	*Glytoconus floweri*	Nfld.	495	0.708958
Z4 32/3	Boat Hbr.	*Rossodus manitouensis*	Nfld.	499	0.708960
Z4 32/2	Boat Hbr.	*Acanthodus uncinatus*	Nfld.	499	0.708955
Z4 32/1	Boat Hbr.	*Clavohamulus renuliformis*	Nfld.	499	0.708967
Z4 18	Watts Bight	*Variabiloconus bassleri*	Nfld.	503	0.708995
Z2 3B	Watts Bight	*Clavohamulus neoelongatus*	Nfld.	507	0.709024
Z7 2C	Watts Bight	*Teridontus nakamurai*	Nfld.	510	0.709065